

# Bayesian Networks Analysis of Malocclusion Data

Marco Scutari<sup>1</sup>, Pietro Auconi<sup>2</sup>, Guido Caldarelli<sup>3,4,5,\*</sup>, and Lorenzo Franchi<sup>6,7</sup>

<sup>1</sup>Department of Statistics, University of Oxford, 24-29 St Giles' Oxford OX1 3LB, UK

<sup>2</sup>Private Practice of Orthodontics, Roma, Italy

<sup>3</sup>IMT School for Advanced Studies, Piazza San Francesco 19, 55100 Lucca, Italy

<sup>4</sup>Istituto dei Sistemi Complessi CNR, Unità Sapienza, Dip. Fisica, P.le A. Moro 2, 00185 Rome, Italy

<sup>5</sup>London Institute for Mathematical Sciences, 35a South St, Mayfair London W1K 2XF, UK

<sup>6</sup>Dipartimento di Ortodonzia, Università di Firenze, Firenze, Italy

<sup>7</sup>Center for Human Growth and Development, University of Michigan, Ann Arbor MI, USA

\*Guido.Caldarelli@imtlucca.it

## ABSTRACT

In this paper we use Bayesian networks to determine and visualise the interactions among various Class III malocclusion maxillofacial features during growth and treatment. We start from a sample of 143 patients characterised through a series of a maximum of 21 different craniofacial features. We estimate a network model from these data and we test its consistency by verifying some commonly accepted hypotheses on the evolution of these disharmonies by means of Bayesian statistics. We show that untreated subjects develop different Class III craniofacial growth patterns as compared to patients submitted to orthodontic treatment with rapid maxillary expansion and facemask therapy. Among treated patients the CoA segment (the maxillary length) and the ANB angle (the antero-posterior relation of the maxilla to the mandible) seem to be the skeletal subspaces that receive the main effect of the treatment.

## Introduction

The use of statistical methods in medicine is crucial to overcome the large individual variability in the pathological features of different patients.<sup>1</sup> In the orthodontic discipline, the variability of craniofacial disharmonies is especially relevant due to important differences between individuals in the amount and direction of facial growth due to heredity, gender, ethnic background, and functional characteristics.<sup>2</sup> In this paper we introduce an approach based on modern techniques from Bayesian statistics for Complex Network analysis to estimate and describe the evolution of orthodontic features measured simultaneously on a set of patients. An incredibly large amount of integrations of the various components of the craniomaxillary and mandibular combinations are possible during the growth process: the integration of these features determines the ultimate dentofacial harmony or disharmony.<sup>3</sup> An in-depth understanding of the resulting large amounts of interrelated data obtained from clinical, radiographic, and functional analyses is required to establish a solid knowledge basis for orthodontic diagnoses. Malocclusions are isoforms of disharmony: they express a form of organic integrity during the growth process by assimilating existing elements in a new synthesis. These isoforms incur costs in terms of weakness of mechanotransduction, cumulative occlusal trauma, adaptability, local optimization, competition between tooth element for space, and outcome uncertainty about the ultimate facial appearance.<sup>4</sup> These conditions are rarely a consequence of an abnormality in a single craniofacial component, so individual clinical and radiological measurements are likely to be less indicative than the interplay between the measurements themselves. In the case of patients affected by Class III malocclusion (characterised by the protrusion of lower dental arch), skeletal imbalance is established early in life, becomes more pronounced during puberty, and continues to increase until skeletal maturation is complete.<sup>4</sup> Therefore, predicting treatment success or failure early in a single Class III patient based on a small number of morphometric determinants is problematic.<sup>5</sup>

Here we present a methodology that makes use of longitudinal data collected from a sample of orthodontic patients to evaluate possible causal paths linking orthodontical features during the growth process and the changes in those paths induced by the treatment. Practising orthodontists often perform clinical reasoning under uncertainty about facial growth, with incomplete information, receiving far more inputs than they can consciously consider; and as a result they are forced to distill clinical and/or radiological evidence into regularities and patterns.<sup>6</sup> Modern techniques in computational statistics build on fundamental principles of probability theory<sup>7</sup> to provide tools for a better understanding and visualisation of complex data by learning those regularities and patterns directly from the data, thus producing rigorous yet tractable models of domains in which very heavy calculation are required for quantitative reasoning.<sup>8</sup> In particular, Bayesian statistic<sup>9,10</sup> develops the idea of combining the information contained in experimental data with prior knowledge available from the literature and from previous

experiments to evaluate the probability of specific hypotheses; an approach that is natural and especially useful in biological and medical research.<sup>11,12</sup> These computational tools can summarise a biological system involving multiple interacting components into a simplified representation that captures the interplay between those components, and that can extract insight about how they influence (and possibly be causal for) each other.<sup>13</sup> A convenient device to represent such complex patterns of relationships are complex networks,<sup>14</sup> which provide a high-level, abstracted view of the interplay between the variables of interest by representing them as nodes and by linking them with arcs that show how those variables interact with each other. A popular choice for this kind of representation are Directed Acyclic Graphs (DAGs), in which links represent direct probabilistic dependencies and have arrows indicating the direction of the dependence. In this paper we intend to develop such a model in the context of orthodontics, combining DAGs with the joint probability distribution of the craniofacial variables of interest.<sup>15</sup> The contribution of DAG's in this case is to visualise the set of relationships between these variables and to determine how they may be grouped into communities. Networks have already been used in the literature to describe the evolution of patients with malocclusions<sup>16</sup> and to help in the formulation of diagnosis.<sup>17</sup> Indeed, the exact focal morphological areas of the treatment effect and treatment priorities are both still under discussion in the clinical orthodontics community.

Unfortunately, the current evidences have been proved unable to fully elucidate the network of causalities that link the relevant skeletal components, the starting point of the treatment, treatment priorities, and the best way to channel and disseminate the effects of the treatment.<sup>17</sup> Here we will try to address such questions for Class III malocclusion, a dysmorphism characterised by growth excess of the mandible and/or a defective growth of the maxilla, with protrusion of the lower dental arch. To this end we will use a set of 147 longitudinal measurements of various craniofacial features on 143 Class III growing patients evaluated at least twice between the ages of 6 and 19. Sixty-six of these subjects were undergoing orthodontic treatment by early rapid maxillary expansion and facemask therapy followed by fixed appliances (2,5), while the remaining 77 were not subject to any treatment. We will estimate Bayesian networks from these data and we will use resampling techniques from modern statistics to produce a consensus network model that describes the relationships between treatment and craniofacial figures and to evaluate its predictive accuracy. We find the resulting network to be consistent with a number of key characteristics of Class III malocclusion as known from current clinical evidence and literature, which we use to validate the relationships we learn from the longitudinal data. Furthermore, the network displays good predictive accuracy for the dynamics of Class III malocclusion in new patients. Finally, we use the network to identify the focal morphological areas of the treatment effect on the basis of the causal relationships captured by the network structure.

## Methods

### The Data

The data contain longitudinal measurements on a set of 147 Class III growing patients evaluated at least twice between the ages of 6 and 19 (83 female, 60 male). Two sets of simultaneous measurements at ages  $T_1$  (6 to 19 years, average  $8 \pm 1$  years) and  $T_2$  (5 to 19 years, average  $15 \pm 1$  years) are available for all patients, in addition to a *Treatment* variable identifying treated from untreated patients. For each untreated subject, a *Growth* variable indicating the prognosis as positive or negative in comparison with the normal craniofacial progression was reported. The complete list and details for the 8 variables for this data set can be found in the Supplementary Information.

### Correlation Networks

We represent the entire craniofacial system as an aggregate structure of a variety of agents where the clinical (e.g., radiographic, functional) features that are the vertices of a network whose edges are the relationship between them. To build the network we start from the measure of correlation among the cephalometric variables  $X_a, X_b$  and in particular we compute the Pearson Correlation coefficient  $r$  defined as

$$r = \frac{\sum_{i=1}^n (X_a(i) - \bar{X}_a) (X_b(i) - \bar{X}_b)}{\sqrt{\sum_{i=1}^n (X_a(i) - \bar{X}_a)^2} \sqrt{\sum_{i=1}^n (X_b(i) - \bar{X}_b)^2}} \quad (1)$$

where  $X_a(i)$  is the  $i$ -th value of the feature  $X_a$  as observed in the data. Once this is computed we keep only the values above the threshold of 0.4, those ones form the edges of the network.

### Bayesian Statistics

The field of statistics provides several approaches to estimate the probability of particular events of interest and to model the laws that govern the phenomena under investigation. For instance, we can estimate the former with its observed, empirical frequency (*frequentist statistics*); and the latter by making assumptions on the distribution of the data and estimating the values of the parameters of the model as those that are best supported by the data (that is, having the maximum *likelihood*).<sup>18</sup> A third approach is given by *Bayesian statistics*,<sup>19</sup> in which we also assume *a priori* a distribution for the parameters of the model.

That distribution is then updated based on the observed data to reflect the current understanding of the phenomenon; the result is the *posterior distribution* of the parameters given the data. For instance, consider the probability  $p(e|c_i)$  of the occurrence of an event  $e$  we observe under one of several possible conditions  $c_i, i = 1, \dots, k$ . A classic approach in statistics is to estimate  $p(e|c_i)$  by means of its frequency (the ratio of how many times the event is observed over the total number of measurements), and then to diagnose the condition as that that has the largest  $p(e|c_i)$ . On the other hand, Bayesian statistics answer a different question, what is the probability of each condition  $c_i$  given the event  $e$ ? Using Bayes theorem, we can write

$$p(c_i|e) = \frac{p(e, c_i)}{p(e)} = \frac{p(c_i)p(e|c_i)}{p(e)} = \frac{p(c_i)p(e|c_i)}{\sum_{j=1}^k p(c_j)p(e|c_j)} \quad (2)$$

to express the *a posteriori* probability of  $c_i$  as a function of the *a priori* probability  $p(c_i)$  of the condition and  $p(e|c_i)$  relative that of the complete set of conditions. As a result, we obtain a completely specified probabilistic model we can use to test experimental hypotheses and that can easily incorporate additional information available from external sources via the  $p(c_i)$  terms. Importantly, this makes it possible to iteratively update  $p(c_i|e)$  as new data becomes available by taking the current estimates of  $p(c_i|e)$  as the *a priori*  $p(c_i)$  for the new data to compute new, up-to-date estimates of  $p(c_i|e)$ .

### Differential Equations Models

Since we are interested in modelling the evolution of malocclusion and its response to treatment over time, we will model the data using the differences of the craniofacial features between different time points instead of the point raw measurements. We assume that each difference can be modelled with a linear regression<sup>20</sup> of the form

$$\Delta Y = \mu + \Delta T \beta_1 + \Delta X_1 \beta_2 + \dots + \varepsilon_{\Delta Y} \quad (3)$$

where  $\varepsilon_{\Delta Y} \sim N(0, \sigma_{\Delta Y}^2)$ ,  $\Delta T = T_2 - T_1$  and  $\Delta Y = Y_{T_2} - Y_{T_1}$  and so forth for the other regressors. We can then rewrite Eq. 3 as

$$\frac{\Delta Y}{\Delta T} = \mu^* + \frac{\Delta X_1}{\Delta T} \beta_2^* + \dots + \varepsilon_{\frac{\Delta Y}{\Delta T}} \quad (4)$$

which in the limit of  $\Delta T \rightarrow 0$  can be considered as a set of differential equations that models the rates of change. (This is a particular case of structural equation models,<sup>21</sup> which are widely used in statistical genetics and systems biology.<sup>22,23</sup>) The relationships between the differences are assumed to be well approximated by a linear behaviour. This constraint is intrinsically enforced by the data: only 120 out of 147 patients have been measured only twice, making it impossible to estimate any trend more complex than linear. Note that Eq. 3 and 4 imply that craniofacial features change linearly over time, because each rate of change  $\Delta Y / \Delta T$  depends on the rates of change of other variables but not on time itself. To have a nonlinear trend we would need

$$\Delta Y = \mu + \Delta T \beta_1 + (\Delta T)^2 \beta_2 + \dots \quad \implies \quad \frac{\Delta Y}{\Delta T} = \mu^* + \Delta T \beta_2^* + \dots \quad \implies \quad \frac{\Delta Y}{\Delta T^2} = \beta_2^* \neq 0. \quad (5)$$

Furthermore, including the *Growth* and *Treatment* in the differential equations makes it possible to have regression models of the form

$$\frac{\Delta Y}{\Delta T} = \mu^* + \frac{\text{Growth}}{\Delta T} \beta_G^* + \frac{\text{Treatment}}{\Delta T} \beta_{TR}^* + \frac{\Delta X_1}{\Delta T} \beta_2^* + \dots + \varepsilon_{\frac{\Delta Y}{\Delta T}} \quad (6)$$

thus allowing for different rates of change depending on whether the patient shows positive developments or not in the malocclusion and whether he is being treated or not. Conversely, we do not allow the treatment level to depend on  $\Delta T$ , since patients are either treated or untreated for the whole period of observation; and we do not assign a regression model to  $\Delta T$  because we assume that it does depend on any measured variables.

### Bayesian Networks

A Bayesian network<sup>24,25</sup> is a statistical model to describe probabilistic relationships among a set of variables using a directed acyclic graph (DAG). The global distribution of the variables  $\mathbf{X} = \{X_1, \dots, X_p\}$ , where  $p$  is the number of different features (in this case  $p = 9$ ) is decomposed into a the local distributions of the individual variables  $X_i$  as

$$p(\mathbf{X}) = \prod_{i=1}^p p(X_i | Pa(X_i)) \quad (7)$$

where  $p(X_i | Pa(X_i))$  are the variables that correspond to the parents of  $X_i$  in the DAG (i.e. the nodes with an arc pointing towards  $X_i$ ). The process of estimating such model is called *learning*, and consists in two steps:

- “learning” which arcs are present in the graph (i.e. which probabilistic relationships are supported by the data);
- “learning” the parameters that regulate the strength and direction of those dependencies.

The former is known as *structure learning*, and the latter as *parameter learning*. In the context of the differential equations described above in Eq. 3, in structure learning we determine which regressors (if any) are present in each of the differential, while in parameter learning we estimate the values of the corresponding regression coefficients. In order to do that, we assume that the errors in each differential equation (represented by the  $\epsilon_{\Delta Y}$  term) are normally distributed, independent, homoscedastic and with mean zero. Under these assumptions, each differential equation can be treated as a classic linear regression model and estimated in the usual way; and the regressors correspond to the variables associated to the nodes that are parents of  $\Delta Y$  in the DAG.

Structure learning is similarly based on model selection procedures for classic regression models. Since we operate in a Bayesian setting, we select which variables are statistically significant regressors in each differential equation as those that maximise the posterior probability of the Bayesian network, which we approximate with the *Bayesian Information Criterion*.<sup>26</sup> Those regressors are the parents of the node corresponding to the response variable in the DAG, and are chosen using hill-climbing, a greedy search algorithm based on step-wise selection.<sup>27</sup> The only restriction imposed by Bayesian networks is that, once the probabilistic relationships are represented as a directed graph, the graph should be acyclic.

While it is possible in principle to learn all dependencies from the data, Bayesian networks can easily include prior knowledge available from the literature and the practice of the discipline to produce more informative models and to overcome the inherent noisiness of orthodontic data. This can be done by encoding the available prior knowledge in sets of arcs whitelisted arcs (which we know represent real dependencies and thus should be forced to be present in the graph) and blacklisted arcs (which correspond to relationships we know to be impossible). In particular:

- Craniofacial features do not determine  $\Delta T$  and *Treatment*, so we blacklist any arc from the former to the latter. We also blacklist any arc from the craniofacial features to *Growth*, as we interpret them to be determined by the overall evolution of the malocclusion (including unobserved factors) as expressed by *Growth*. This also leads to a more intuitive parameterisation of the differential equations, with different regimes for the craniofacial features depending on the prognosis.
- We blacklist any arc from  $\Delta T$  and *Treatment* as discussed above.
- We whitelist the dependence structure  $\Delta ANB \rightarrow \Delta IMPA \leftarrow \Delta PPPM$ .<sup>1,4,5</sup>
- We whitelist the arc from  $\Delta T$  to *Growth* to allow the prognosis to change over time.

We want to clarify the meaning of the variable “Growth” that we used in our analysis: Growth, is a parameter that reflects the prognosis, done to the patient, at the time of the visit. In such respect this is a “static” variable and does not reflect a measure of the effective growth. Quality of growth has been evaluated by considering the normal evolution of the maxillomandibular sagittal imbalance (CoGn-CoA) with respect to average population. Patients near the average values were diagnosed as “good growers” while the others were indicated as “bad growers”.<sup>28</sup> Furthermore, to reduce the impact of the noise present in the data, we use a second Bayesian technique called *model averaging* to improve the reliability of structure learning.<sup>29</sup> Typically, to examine the phenomenon under investigation we estimate a single model from the data, and we draw our conclusions from that model treating it as a “fixed” quantity. This traditional approach underestimates the degree of uncertainty in those statistical conclusions by ignoring the fact that the estimated model is not “fixed”, but carries its own uncertainty from the selection procedure used to identify it as the optimal model for the data.<sup>30</sup> Intuitively, we can imagine that adding or removing a few observations from the data may result in a different model being identified, in turn leading to different conclusions. To reduce this model uncertainty, we re-sample the data 200 times using bootstrap<sup>31</sup> and we perform structure learning separately on each of the resulting samples, thus collecting 200 DAGs. We then compute the frequency with which each appears in those 200 graphs, known as *arc strength* and we compute an “average”, consensus DAG by selecting those arcs that have a frequency above a certain threshold. (The threshold can either be estimated from the data or set to an arbitrary value, such as 0.85 below, for the purpose of obtaining a sparse DAG that is easier to interpret.) The averaged Bayesian network model has a number of favourable statistical properties; in particular, it is less sensitive to noisy data and typically produces more accurate predictions for new observations.

Once we have estimated the average Bayesian network and the values of the regression coefficients in the differential equations it describes, we evaluate its predictive accuracy using 10-fold cross-validation.<sup>32</sup> 10-fold cross-validation is a model validation technique that assesses how well a statistical model generalises to independent data or, in other words, how accurately it will predict the behaviour of new observations. It is implemented as follows.

1. We split the data into 10 subsets (called “folds”) of the same size (or as close as possible).

2. For each fold in turn:
  - (a) we take that fold as the *test set*;
  - (b) we take the rest of the data as the *training set*;
  - (c) we learn the Bayesian network model on the training set, both the structure and the parameters;
  - (d) we predict each variable in turn for the observations in the test set, from the model we learned from the training set and from all the other variables in the test set;
3. We collect the pairs of (observed, predicted) values for all the observations and:
  - (a) for each continuous variable, we compute the correlation between the observed and predicted pairs (this quantity is called *predictive correlation*);
  - (b) for Growth, we compute the number of misclassified predicted values using the observed values as the true values (this is the *predictive classification error*, which the complement of predictive accuracy).

In addition, we use the averaged Bayesian network for inference to check answer a number of crucial questions and to check whether it reflects the available knowledge of how the measured variables interact with each other and with the treatment. In the context of Bayesian networks, this is typically done using a technique called *belief updating*, in which we estimate the posterior probability of a certain event or the posterior estimate of some parameter conditional on some evidence on the values of one or more variables. Several exact and approximate approaches are available in the literature;<sup>25</sup> in this paper we use logic sampling for its simplicity. Logic sampling is defined as follows:

1. Define a counter  $n_E = 0$  for the evidence and a counter  $n_q = 0$  for the event of interest;
2. For a suitably large number of times ( $10^4$ – $10^6$ ):
  - (a) generate a random sample from the Bayesian network.
  - (b) if the random sample matches the evidence, set  $n_E = n_E + 1$ ;
  - (c) if the random sample matched both the evidence and the event, set  $n_{E,q} = n_{E,q} + 1$ .
3. Estimate the conditional probability of the event given the evidence with  $n_{E,q}/n_E$ ; or compute the posterior estimates of the parameters of interest using those random observations that match the event.

By applying this approach we can answer arbitrary questions, which are called *conditional probability queries*, from a Bayesian network. We perform the whole analysis using the bnlearn package<sup>15</sup> for R.<sup>33</sup>

## Results

### Raw data

As discussed in the literature,<sup>16,17</sup> craniofacial features evolve and respond to external stimuli as a system and therefore they form clusters of variables with high (greater than 0.40 in absolute value) pairwise Pearson's correlation. one characterising the vertical divergence of the maxillo-mandibular structure (*ArGoMe*, *PPPM* and *SNGoGn*), one composed by sagittal and adaptive variables (*ANB*, *Wits*, *Overjet*, *IMPA*), and one composed by skeletal and basiocranial features (all other variables with the exception of *NSar* and *PPSN*, which are not connected to any other variable). Using partial Pearson's correlation (i.e. the correlation of each pair of variables after all other variables have been taken into account through conditioning) provides a clearer pictures of which craniofacial features are directly related. The two resulting clusters are shown in Fig. ?? : a first one including *SNA*, *SN*, *NSar*, *SNB*, *PPPM*, *PPSN*, *SAr* and *CoGn*; and a second one including *CoA*, *NMe*, *ArGoMe*, *GoPg*, *SNGoGn*, *IMPA* and *FMIA*. Other variables are only weakly correlated with those two clusters and appear as isolated nodes in the graph. In this network the adaptive nodes *IMPA* and *FMIA* are strictly connected with vertical imbalance nodes (*SNGoGn*, *ArGoMe*) in Fig.2, while in the former network the process is mainly directed toward the horizontal skeletal imbalance (*ANB*, *Overjet*, *SNB* nodes) (Fig.1). The Bayesian network consensus model constructed by learning 200 networks from the first data set and keeping the arcs that appear at least 50% of the time (threshold estimated from the data) is shown in Fig. 2. All the directions of the arcs seem to be well established; this can probably be attributed to the use of a whitelist and a blacklist, as they



force the directions of nearby arcs to cascade into place. Furthermore, a cursory examination of the arc strengths above the threshold confirms that 15 out of 18 arcs in the consensus network appear in fact with a frequency of at least 0.85. All arc directions are also clearly established (all frequencies are equal to 1). This allows to further simplify the consensus network as shown in Fig. 3 while losing little information in the process. While the skeletal growth process influence the evolution of sagittal maxillomandibular imbalance (dANB) and mandible ramus height (dCoGo), the treatment effects mainly influence the maxillary length growth (dCoA), and the progression of maxillomandibular imbalance (dANB).

To further validate the Bayesian network, we check whether this is consistent with prior information on Class III malocclusion that has not been used in the construction of the model. We formulate this consistency testing four hypotheses, and we use simulation as described in the Methods to validate it.

1. In Class III growing subjects an excessive growth of *CoGo* induces a reduction in *PPPM*, assuming no treatment is taking place. In the differential equations in the network, we have that as  $\Delta CoGo$  increases (which indicates an increasingly rapid growth)  $\Delta PPPM$  becomes increasingly negative (which indicates a reduction in the angle). This is shown in Fig. 4.
2. In Class III growing subjects if *ANB* decreases, *IMPA* decreases to compensate;  $\Delta ANB$  is proportional to  $\Delta IMPA$ , as shown in Fig. 5, so a decrease in one suggests a decrease in the other.
3. Since Class III orthodontic treatment is aimed at stopping the decrease of *ANB* ( $\Delta ANB \approx 0$ ), we expect to observe different dynamics for *ANB* in treated and untreated patients. First, we note that the Bayesian network correctly assigns a higher probability of a favourable prognosis to treated (0.63) compared to untreated (0.51) patients. The unfavourable prognosis of treated patients was defined as the concurred presence of Class III permanent molar relationship and negative overjet.<sup>34</sup> If we simulate the treatment effect and fix  $\Delta ANB \approx 0$  (thus making it independent from its parents and removing the corresponding arcs), we have that the probability of a favourable prognosis is the same (0.58) for both treated and untreated patients and thus it does not depend on the treatment. This suggests that a favourable prognosis of a Class III malocclusion is mainly determined by preventing changes in *ANB*.
4. If we use *GoPg* as a proxy for point B, the treatment does not affect point B after controlling for point A: if we keep *GoPg* fixed ( $\Delta GoPg \approx 0$ ) the angle between point A and point B ( $\Delta ANB$ ) evolves differently for treated and untreated patients. On average,  $\Delta ANB$  increases for treated patients (+0.37 degrees; strongly negative values denote horizontal imbalance, so a positive rate of changes indicate a reduction in imbalance) and decreases for untreated patients (−1.13 degrees; the imbalance slowly worsens over time).

Finally, we also consider the predictive accuracy of the consensus Bayesian network. Using cross-validation as described in the Methods, we find that the prognosis is accurately predicted with probability 0.73. The predictive correlations for the craniofacial features are 0.86 for  $\Delta CoGo$ , 0.91 for  $\Delta GoPg$ , 0.92 for  $\Delta CoA$ , 0.23 for  $\Delta IMPA$ , 0.42 for  $\Delta PPPM$  and 0.65 for  $\Delta ANB$ .

We also learn two separate consensus Bayesian networks from treated and untreated patients, which are shown Fig. 8. There are significant differences between the influence networks pertaining to treated and untreated subjects. The treatment effects on the craniofacial subspaces are channeled through the maxillary node *CoA* to the mandibular nodes *CoGo* (mandibular ramus) and *GoPg* (mandibular body). The adaptive *IMPA* node (which aims to maintain unchanged the sagittal relationship between the maxilla and the mandible) is influenced by both horizontal and vertical skeletal imbalances during the treatment process (i.e., by dPPPM and dANB). On the contrary, among Class III untreated subjects the progression of the horizontal skeletal imbalance (dANB) strictly influences the maxillary node *CoA*, which in turn influences the progression of mandibular nodes *GoPg* and *CoGo* during the growth process.

## Adjusted data

With the aim of confirming the methodological approach we introduced in this paper, we just considered another case of study. This is obtained by considering an Atlas of normal cephalometric features<sup>2</sup> during infancy and childhood and used adjusted data for the same variables, with values adjusted by subtracting the corresponding reference values from the Atlas. A consensus Bayesian networks built in the same way as that for the raw data is shown in Fig. 7. The threshold for the significance of the arcs is about the same as before (0.5) and the number of arcs is also similar. The most striking feature of avg.simpler is the lack of arc between dT and any of the orthodontic variables; the only arcs from dT points to Growth and is only included because of the whitelist. (Note that the same happened when we excluded the individuals with the most extreme dT, and the networks in the two cases are very similar.) This seems to suggest that much of the dependence on dT observed in the raw data is not a consequence of the evolution of the malocclusion but a result of ageing. This is consistent with the fact that if we reduce the spread in the observed ages by bounding dT, most of the dependencies on dT vanish. We can conjecture that the nonlinear trend of the raw values of the orthodontic variables (that is, the fact that their rate of change is a function

of time) can be decomposed into two components: a general population average and a deviation from that average given the malocclusion. The former effectively changes with time (that is, the trend of the population mean over time is not constant) while the latter does not (that is, the rate of change of the deviation from the population mean depends only on other orthodontic values and on the treatment). In other words, the population average evolves with age for all orthodontic variables, which is expected as the patients are not yet fully grown adults. However, the deviations from the populations averages do not seem to evolve with age, or to be a function of the passage of time. This would imply that the effects applying a change to one of the orthodontic variables propagate to related orthodontic variables and cause them to respond them in the same way regardless of how quickly the change is applied. (e.g. a one-degree shift in ANB influences neighbouring variables such as CoA and IMPA in the same way regardless of how quickly that one-degree change happens; it can be one year, it can be two years, etc. but those neighbouring variables will have the same value at the end).

We consider the predictive accuracy of this new consensus Bayesian network, using cross-validation as we did for the network we learned from the non-adjusted data. We find that the probability of correctly predicting the prognosis is similar (0.74 vs 0.73). The predictive correlations for most craniofacial features, however, are smaller: 0.64 (−0.22) for  $\Delta CoGo$ , 0.68 (−0.23) for  $\Delta GoPg$ , 0.81 (−0.11) for  $\Delta CoA$ , 0.28 (+0.05) for  $\Delta IMPA$ , 0.39 (−0.03) for  $\Delta PPPM$  and 0.71 (+0.06) for  $\Delta ANB$ . This is expected since we are now modelling deviations from the population average, which are intrinsically more difficult to analyse.

We also learn two separate consensus Bayesian networks from treated and untreated patients, which are shown Fig. 6. Among both untreated and treated subjects the progression of skeletal imbalance is influenced by the evolution of the maxillary sagittal dimensions (dCoa); however, only treated patients exhibit the strong dependency of the mandibular corpus from dCoA.

## Discussion

Previous studies have proposed different cephalometric models to determine specific facial parameters related to abnormal growth patterns in Class III untreated and treated patients.<sup>2,4,5</sup> Multilevel, nonparametric, and predictive function algorithms have provided growth predictions and treatment outcomes based on a variety of facial characteristics.<sup>4,5</sup> Recently, network approaches to understanding morphological and functional relationships among orthodontic data have been proposed.<sup>16,17</sup> While this approach improved the interpretation of the quantitative, patient-specific information, networks were unable to elucidate the effects of influences (possibly, causal influences) between craniofacial variables.<sup>16</sup> Craniofacial features change and adapt as a system in response to both natural stimuli such as growth and external stimuli such as clinical treatments. This implies that efforts towards understanding diseases such as malocclusion must reflect this interplay in the choice of statistical models and in how clinically relevant hypotheses are tested. This has motivated the use of network approaches<sup>16,17</sup> which represents features as nodes in an undirected graph and explicitly groups them into clusters based on their pair-wise correlation. These clusters describe particular regions of the craniomaxillary and mandibular complexes and other broad features (symmetry, proportions, etc.) that are impacted by malocclusion and that must be targeted by treatment.

This modelling approach, however, has three important limitations. The first is that the use of pair-wise correlations makes it impossible to distinguish direct relationships between two features from indirect ones that are mediated by other features, thus making it difficult to get a clear picture of system as a whole and to identify the best target for the treatment.<sup>35</sup> Furthermore, the direction of the relationships is not taken into consideration by the model nor it is represented in the graph, making it impossible to infer cause-effect relationships even in the presence of data systematically collected from a clinical trial.<sup>13</sup> Finally, limiting the model to a representation of pair-wise dependencies falls short of characterising the full probability distribution of the features, and that in turn makes it impossible to use it to test the complex hypotheses required for model validation and treatment evaluation.

Bayesian networks suffer from none of these limitations.<sup>12</sup> Thanks to their modular model structure and to the availability of efficient software implementations,<sup>15</sup> they can be used to simultaneously explore a large number of features. The number of features does not impact the interpretability of the network: focusing on direct dependencies means that each feature is described by a local distribution that depends only those features (the “parents”) for which the corresponding nodes have an arc with an arrow pointing to that particular feature. Therefore, complex models are split into a collection of simpler problems which are mathematically tractable and computationally simpler. Furthermore, the DAG can always be used as a high level abstraction for qualitative reasoning in the context of exploratory analysis and to investigate hypotheses on the whether various sets of features are related to each other.<sup>24</sup> Finally, a Bayesian network can also be interpreted as a causal network in the absence of confounding factors<sup>13</sup> and used to examine or generate novel clinical hypotheses.<sup>36</sup> The inherently Bayesian nature of a Bayesian network facilitates such reasoning by incorporating both prior knowledge about the variables of interest and the uncertainty present in the data;<sup>37</sup> and by not defining model estimation and inference around a single response at the expense of the ability to reason about other variables (unlike, e.g., linear regression models).

However, information becomes knowledge only when it is placed in context: without it, the orthodontist has not way to differentiate the signal from the noise, so the research for better diagnosis and treatment might be swamped by false positives

and false assumptions. In some situations of daily practice, the orthodontist's efforts are aimed (or perhaps compelled), to the optimization of therapy more than the optimization of diagnosis. The result is that the therapy is effective, sometimes extraordinarily effective, but the price of a hasty diagnosis is paid in terms of relapse of the pretreatment craniofacial features. The aim of this work is therefore to obtain an integrated view of the craniofacial features, the treatment and the prognosis to allow systematic reasoning in the diagnostic process.

The use of Bayesian networks allows us to achieve this aim. We identify the focal morphological areas of the treatment for Class III malocclusion as the *CoA* segment (the maxillary length) and the *ANB* angle (the antero-posterior relation of the maxilla to the mandible); therefore, any apparent effect of the treatment on other cranial features can be disregarded as noise since it is actually mediated by these two features. Furthermore, by modelling the putative causal relationships we can study how the effect of an intervention on one feature propagates by identifying neighbouring features in the DAG and by studying how their distribution changes in response. We performed such and exercise to validate the consensus Bayesian network with respect to prior knowledge on malocclusion, with promising results.

To our knowledge, this is the first time a complex system such as craniofacial features has been modelled in such a way with a formal statistical and causal Bayesian network. The usefulness of such a model is two-fold: it provides an intuitive qualitative description (in the form of a DAG) of the relationships that link the craniofacial features beyond mere physical proximity; and it also provides a quantitative description of their behaviour that can be used to validate the model and to test novel hypotheses by simulation. Collecting clinical data on either treated or untreated in the context of clinical trials is expensive, time consuming and subject to many practical, legal and deontological problems. In this context, Bayesian networks provide a way to perform a preliminary verification of the hypotheses targeted by those trials to prioritise the trials and allocate resources efficiently. For instance, in this paper we identified the focal point of the effect of the facemask therapy. To perform the same task experimentally without the help of the Bayesian network would require us to check many different locations; but with the indications provided by the Bayesian networks we can concentrate on *CoA* and *ANB* first and possibly avoid further experiments involving the remaining features. This sequential approach to experimental design and planning is becoming increasingly common in systems biology to reduce the cost of *in vitro* and *in vivo* research programmes,<sup>38</sup> and by the pharmaceutical industry to reduce the costs and risk of pharmaceutical trials.<sup>11</sup>

While Bayesian networks can deal with the uncertainty in the data, their main limitations lie in the impact of confounding variables and in the assumptions they make about the distribution of the features. With a larger number of measurements per patients, for instance, we expect assuming linear relationships between the features would be a significant limitation, since we would have enough statistical power to detect nonlinear relationships.

The results of this study show that the Bayesian networks applied to a growing craniofacial complex are a useful tool to define a more detailed individualized prognosis for patients affected by the Class III malocclusion, and to mitigate an unpredictable ultimate outcome of this dysmorphosis.

## References

1. Scotch, M., Duggal, M., Brandt, C., Lin, Z. & Shiffman, R. Use of Statistical Analysis in the Biomedical Informatics Literature. *Journal of the American Medical Informatics Association* **17**, 3–5 (2010).
2. Nanda, R. & Uribe, R. A. *Atlas of Complex Orthodontics* (Elsevier, 2016).
3. Zaidel, D. W. & Cohen, J. A. The Face, Beauty, and Symmetry: Perceiving Asymmetry in Beautiful Faces. *The International Journal of Neuroscience* **115**, 1165–73 (2005).
4. Baccetti, T., Franchi, L. & McNamara, J. A. Growth in the Untreated Class III Subject. *Seminars in Orthodontics* **13**, 130–142 (2007).
5. Fudalej, P., Dragan, M. & Wedrychowska-Szulc, B. Prediction of the Outcome of Orthodontic Treatment of Class III Malocclusions—a Systematic Review. *European Journal of Orthodontics* **33**, 190–197 (2011).
6. Silver, N. *The Signal and the Noise: Why So Many Predictions Fail—but Some Don't* (Penguin, 2015).
7. Cumming, G. The New Statistics: Why and How. *Psychological Science* **25**, 7–29 (2014).
8. Pearl, J. *Probabilistic Reasoning in Intelligent Systems: Networks of Plausible Inference* (Morgan Kaufmann Publishers Inc., 1988).
9. Bayes, T. & Price, M. An Essay Towards Solving a Problem in the Doctrine of Chances. *Philosophical Transactions* **1683-1775**, 370–418 (1763).
10. Laplace, P. S. Memoir on the Probability of the causes of Events (1774) Translated from French. *Statistical Science* **1**, 364–378 (1986).
11. Berry, S. M., Carlin, B. P., Lee, J. J. & Müller, P. *Bayesian Adaptive Methods for Clinical Trials* (Chapman & Hall, 2011).



12. Nagarajan, R., Scutari, M. & Lèbre, S. *Bayesian Networks in R with Applications in Systems Biology*. Use R! series (Springer, 2013).
13. Pearl, J. *Causality: Models, Reasoning and Inference* (Cambridge University Press, 2009), 2nd edn.
14. Caldarelli, G. *Scale-Free Networks: Complex Webs in Nature and Technology* (Oxford University Press, 2007).
15. Scutari, M. Learning Bayesian Networks with the bnlearn R Package. *Journal of Statistical Software* **35**, 1–22 (2010).
16. Scala, A. *et al.* Complex Networks for Data-Driven Medicine: the Case of Class III Dentoskeletal Disharmony. *New Journal of Physics* **16**, 115017 (2014).
17. Auconi, P., Caldarelli, G., Scala, A., Ierardo, G. & Polimeni, A. A Network Approach to Orthodontic Diagnosis. *Orthodontics & Craniofacial Research* **14**, 189–197 (2011).
18. Young, G. A. & Smith, R. L. *Essentials of Statistical Inference* (Cambridge University Press, 2005).
19. Lee, P. M. *Bayesian Statistics: an Introduction* (Wiley, 2012), 2nd edn.
20. Weisberg, S. *Applied Linear Regression* (Wiley, 2013), 4th edn.
21. Hoyle, R. H. *Structural Equation Modeling: Concepts, Issues, and Applications* (SAGE, 1995).
22. Li, R. *et al.* Structural Model Analysis of Multiple Quantitative Traits. *PLoS Genetics* **2**, e114 (2006).
23. Rosa, G. J. M. *et al.* Inferring Causal Phenotype Networks Using Structural Equation Models. *Genomic Selection Evolution* **43**, 6 (2011).
24. Koller, D. & Friedman, N. *Probabilistic Graphical Models: Principles and Techniques* (MIT Press, 2009).
25. Scutari, M. & Denis, J.-B. *Bayesian Networks with Examples in R* (Chapman & Hall, 2014).
26. Schwarz, G. Estimating the Dimension of a Model. *The Annals of Statistics* **6**, 461–464 (1978).
27. Russell, S. J. & Norvig, P. *Artificial Intelligence: A Modern Approach* (Prentice Hall, 2009), 3rd edn.
28. Auconi, P. *et al.* Understanding interactions among cephalometrics variables during growth in untreated Class III subjects *European Journal of Orthodontics* (2017). URL <https://doi.org/10.1093/ejo/cjw084>.
29. Scutari, M. & Nagarajan, R. On Identifying Significant Edges in Graphical Models of Molecular Networks. *Artificial Intelligence in Medicine* **57**, 207–217 (2013).
30. Claeskens, G. & Hjort, N. L. *Model Selection and Model Averaging* (Cambridge University Press, 2008).
31. Efron, B. & Tibshirani, R. *An Introduction to the Bootstrap* (Chapman & Hall, New York, 1993).
32. Hastie, T., Tibshirani, R. & Friedman, J. *The Elements of Statistical Learning: Data Mining, Inference, and Prediction* (Springer, 2009), 2nd edn.
33. R Development Core Team. *R: A Language and Environment for Statistical Computing*. R Foundation for Statistical Computing, Vienna, Austria (2016).
34. Auconi, P., Scazzocchio, M., Cozza, P., McNamara, J. A. & Franchi, L. Prediction of class iii treatment outcomes through orthodontic data mining. *The European Journal of Orthodontics* (2014).
35. Opgen-Rhein, R. & Strimmer, K. Learning Causal Networks from Systems Biology Time Course Data: an Effective Model Selection Procedure for the Vector Autoregressive Process. *BMC Bioinformatics* **8** (Suppl. 2), S3 (2007).
36. Lucas, P. J. F., van der Gaag, L. C. & Abu-Hanna, A. Bayesian Networks in Biomedicine and Health-Care. *Artificial Intelligence in Medicine* **30**, 201–214 (2004).
37. Mukherjee, S. & Speed, T. P. Network Inference Using Informative Priors. *Proceedings of the National Academy of Sciences* **105**, 14313–14318 (2008).
38. Pauwels, E., Lajaunie, C. & Vert, J.-P. A Bayesian Active Learning Strategy for Sequential Experimental Design in Systems Biology. *BMC Systems Biology* **8**, 102 (2014).
39. Bathia, S. N. & Leighton, B. C. *A Manual of Facial Growth* (Oxford University Press, 1993).

## Acknowledgments

GC acknowledges support from EU Projects MULTIPLEX (317532).

## Additional information

**Author Contributions** LF and PA collected the data, GC and MS provided the mathematical framework to analyse such dataset. All authors contributed equally to the analysis of the dataset and to the interpretation of the results of this analysis. All authors contributed equally also to the writing of the manuscript.

**Competing financial information** None of the authors has any financial competing interest

# 1 Supplementary Information: Malocclusion Data Analysis

## 1.1 Data

The quantities under consideration are derived from the anatomy of the patient as shown in Fig. 9.

For the data set of 143 patient, we have the following quantities with two measurements at ages  $T_1$  and  $T_2$  (measured in years):

- *ID*: anonymised ID code unique to each patient.
- *Treatment*: untreated (“NT”), treated with bad results (“TB”), treated with good results (“TG”).
- *Growth*: a binary variable with values “Good” or “Bad”, determined on the basis of CoGn-CoA.
- *ANB*: angle between Down’s points A and B (degrees).
- *IMPA*: incisor-mandibular plane angle (degrees).
- *PPPM*: palatal plane - mandibular plane angle (degrees).
- *CoA*: total maxillary length from condilion to Down’s point A (mm).
- *GoPg*: length of mandibular body from gonion to pogonion (mm).
- *CoGo*: length of mandibular ramus from condilion to pogonion (mm).

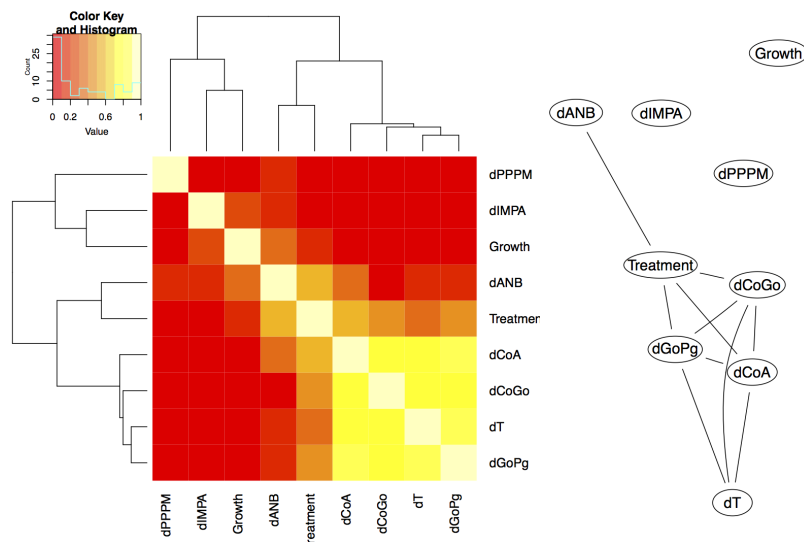


**Figure 1.** (left) A heatmap of the pairwise Pearson's correlation between variables measured on the patients. (right) The undirected graph of displaying pairwise Pearson's correlations greater than 0.40 in absolute value.

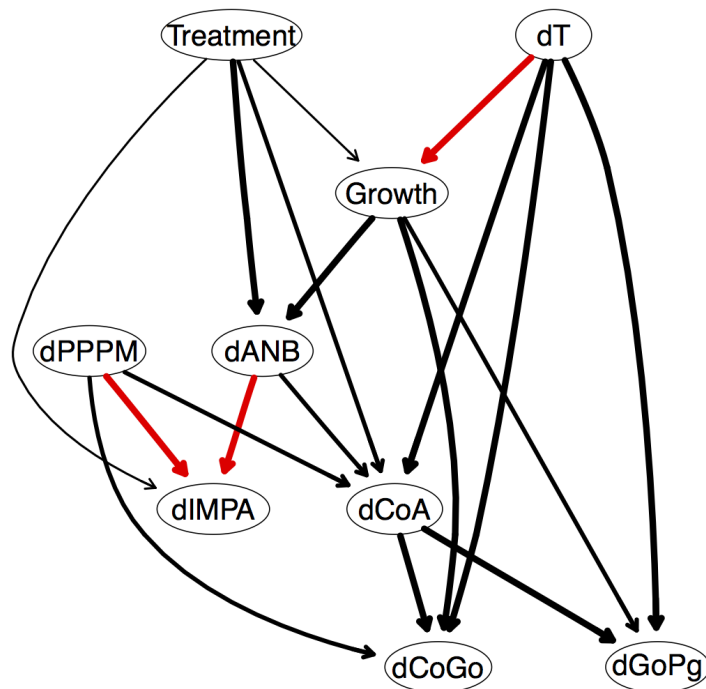


**Figure 2.** The DAG underlying the consensus Bayesian network learned from the variables measured on all 143 patients. Arcs in red are constrained to be present in the network by the whitelist. The thickness of the arcs is in the proportion to their strength; only arcs with a strength greater than 0.5 are included in the consensus network.

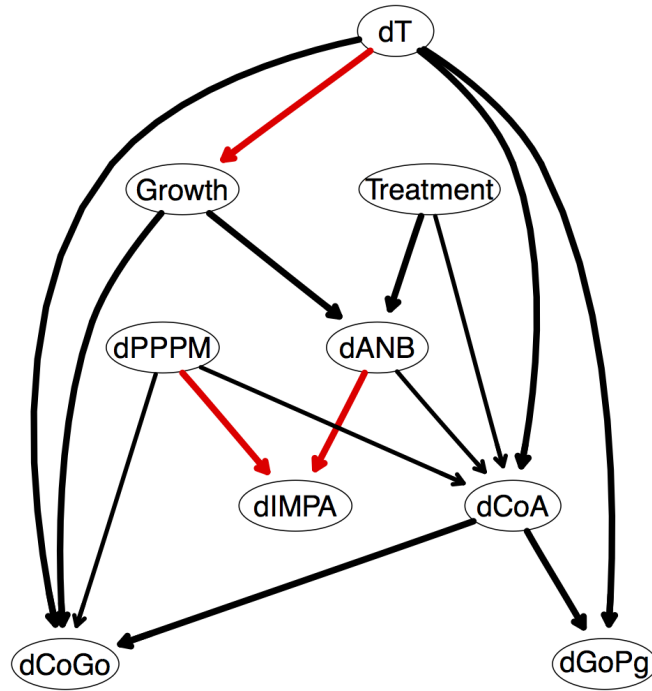


**Figure 3.** A simplified DAG derived from that in Fig. 2 after removing arcs with a strength smaller than 0.85.

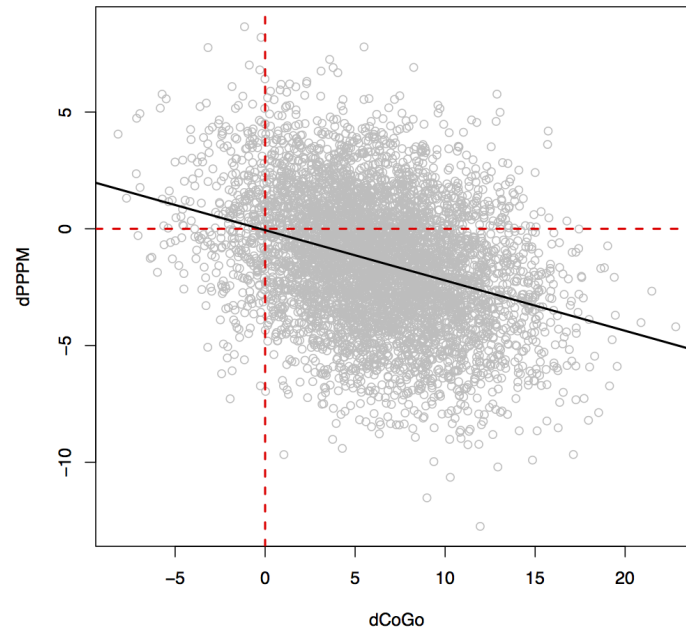


**Figure 4.** Values simulated from the Bayesian network for  $dPPPM$  and  $dCoGo$ . The black line represents the regression line of  $dPPPM$  against  $dCoGo$ ; its negative slope confirms that as  $dCoGo$  increases (which indicates an increasingly rapid growth)  $dPPPM$  becomes increasingly negative (which indicates a reduction in the angle).



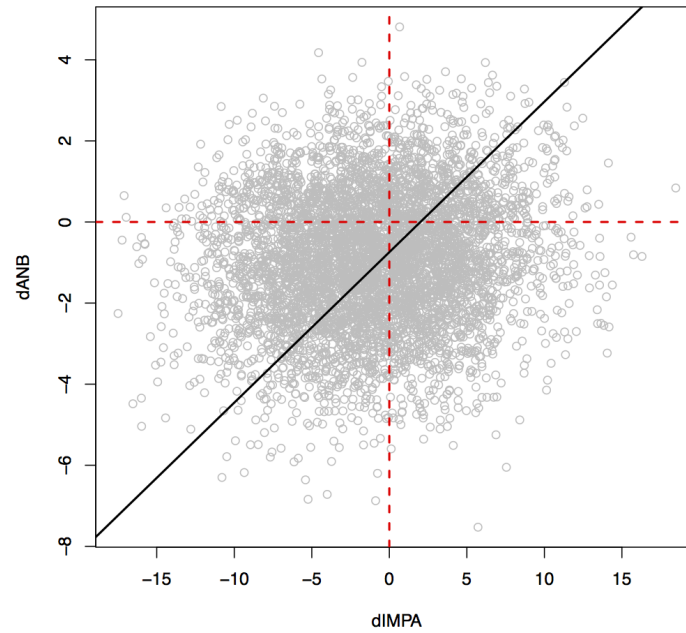


**Figure 5.** Values simulated from the Bayesian network for  $dANB$  and  $dIMPA$ . The black line represents the regression line of  $dANB$  against  $dIMPA$ ; its positive slope suggests that  $dANB$  is proportional to  $dIMPA$ , so a decrease in one suggests a decrease in the other.

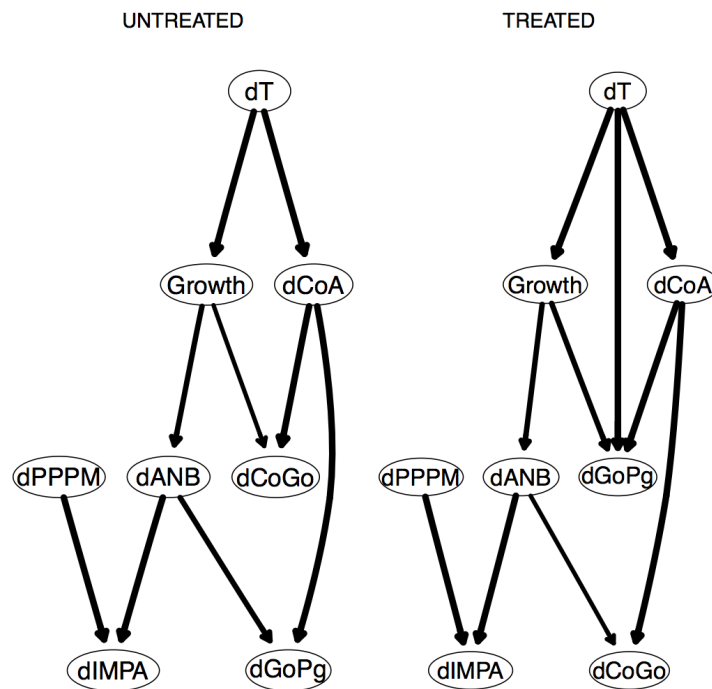


**Figure 6.** The DAGs underlying the consensus Bayesian networks for treated and untreated patients on the 9 variables measured for both.

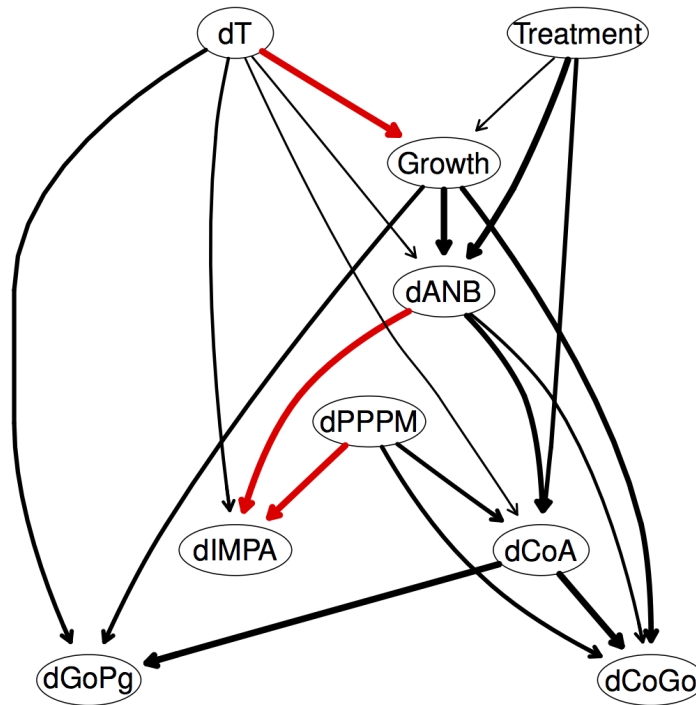


**Figure 7.** The DAG underlying the Bayesian network learned from the 9 variables measured on all 143 patients after adjusting them using the population reference values from Bathia and Leighton.<sup>39</sup>

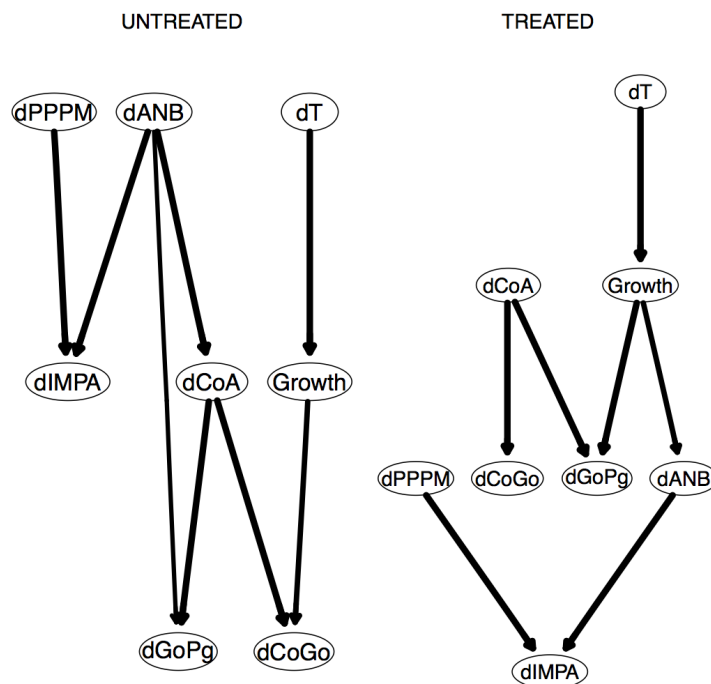


**Figure 8.** The DAGs underlying the consensus Bayesian networks for treated and untreated patients on the 9 variables measured for both, after adjusting them using the population reference values from Bathia and Leighton.<sup>39</sup>

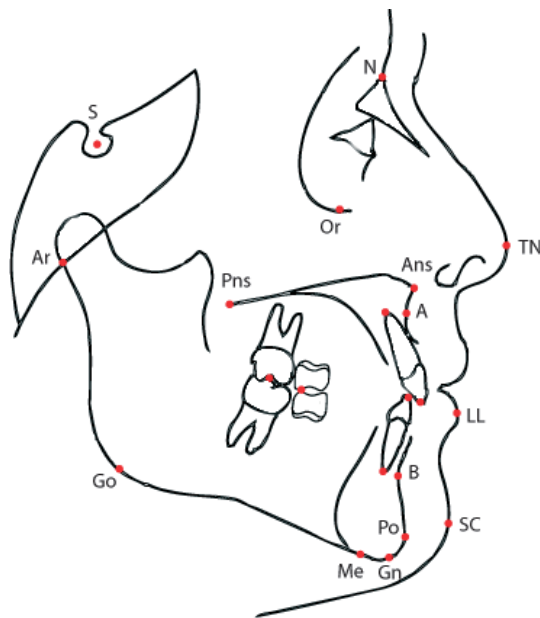


**Figure 9.** Cephalometric landmarks.